Desalination and Water Treatment
www.deswater.com

doi: 10.5004/dwt.2019.24629

167 (2019) 190–199
November

Enhanced photocatalytic degradation of phenol by immobilized TiO_2/dye-loaded chitosan

Sumiyyah Sabar[a,*], Mohd Asri Nawi[b], Ali H. Jawad[c], Raphaël Schneider[d]

[a]*Chemistry Section, School of Distance Education, Universiti Sains Malaysia, 11800 Minden, Penang, Malaysia, Tel. +604 6532284; email: sumiyyahs@usm.my*
[b]*School of Chemical Sciences, Universiti Sains Malaysia, 11800 Minden, Penang, Malaysia, Tel. +6019 4100356; email: masri@usm.my*
[c]*Faculty of Applied Sciences, Universiti Teknologi MARA, 40450 Shah Alam, Selangor, Malaysia, Tel. +603 55211721; emails: ahjm72@gmail.com/ali288@salam.uitm.edu.my (A.H. Jawad)*
[d]*Laboratoire Réactions et Génie des Procédés, Université de Lorraine, CNRS, F-54000 Nancy, France, Tel. +33-3-7274-3790; email: raphael.schneider@univ-lorraine.fr*

Received 5 January 2019; Accepted 30 June 2019

ABSTRACT

In this study, an immobilized TiO_2/dye-loaded chitosan was designed in a layer-by-layer arrangement for the enhanced photocatalytic degradation of phenol under a 45-W compact household fluorescent light irradiation. The immobilized photocatalyst was supported on glass plates and consists of a porous top layer of TiO_2 and sub-layer of chitosan (CS) with chemisorbed Reactive Red 4 (RR4) dye (TiO_2/RR4-CS/glass). Results from the optical studies demonstrated that the absorption threshold of the immobilized photocatalyst was shifted to the visible light region with lower recombination of electron–hole pairs. The TiO_2/RR4-CS/glass exhibits improved photocatalytic degradation and mineralization of phenol as compared with the TiO_2/glass and TiO_2/CS/glass photocatalysts, with a degradation rate of 0.030 min^{-1} and total mineralization of 76.7%. The immobilized photocatalyst also exhibited excellent photocatalytic stability and could be reused for up to five cycles of phenol treatment. The enhanced photocatalytic performance of the TiO_2/RR4-CS/glass can be ascribed to the synergistic photocatalytic and sensitization effects that run concurrently under light irradiation.

Keywords: Chitosan; Dye; Immobilization; Photocatalysis; Sensitization; Titanium dioxide

1. Introduction

Phenol is the most common pollutant emitted into the surface water. It is introduced into water from industries such as pesticides, coal conversion, petroleum, petrochemicals, paint, polymer resin, pharmaceuticals, and also from domestic wastewater. It is a high priority pollutant due to its extremely high endocrine-disrupting potency and genotoxicity even at low concentration [1]. Phenol is water-soluble, stable, and a bio-refractory pollutant which makes its treatment in wastewater by the traditional methods ineffective [2]. Rapid industrialization in Malaysia for the past 20 years has contributed to the increase of phenols in water bodies. In this case, the Department of Environment (DOE) has set a national guideline for phenol content which specifies that its concentration in the wastewater should not exceed 0.001 mg L^{-1} [3]. Therefore, the treatment of phenol-containing wastewater using suitable and efficient method is of high importance.

Photocatalysis is one of the most promising advanced oxidation processes and is a green technology that can be applied to wastewater treatment and water purification.

* Corresponding author.

1944-3994/1944-3986 © 2019 Desalination Publications. All rights reserved.

Titanium dioxide (TiO_2) is considered to be a benchmark semiconductor for photocatalysis not only due to its high activity but also because it is chemically stable, cheap, easy to produce, and environmentally friendly [4]. Under UV light irradiation, TiO_2 produces reactive oxygen species that are able to fully mineralize organic pollutants such as dyes, drugs, pesticides, and phenolic compounds [2,5–7]. However, the high recombination rate of electron–hole pairs and the wide bandgap of TiO_2 (~3.2 eV) restricts its large-scale applications especially under solar and visible irradiation. Hence, it is necessary to modify TiO_2 in order to improve its photocatalytic performances and applicability.

Various methods have been developed to improve TiO_2 photocatalytic activity, including doping with metal ions [7,8], doping with non-metal elements [8,9], building heterojunction with small bandgap semiconductors [10,11], combination with adsorbent [5,12], and dye sensitization [2,6,13–17]. Dye sensitization seems to be an interesting research area since it is the easiest and the most effective technique to improve the visible light sensitivity of TiO_2. Dye absorbs visible light and transfer electrons to the TiO_2 conduction band, thus improving the separation efficiency of photoinduced electron–hole pairs and the photocatalytic activity. In fact, dye-sensitized TiO_2 has received much attention in photovoltaic applications, such as dye-sensitized solar cells [18,19] and photolysis of water to generate hydrogen [20,21]. Various methods have been developed for the preparation of dye-sensitized TiO_2 photocatalytic system. For example, Boyer et al. [13] used cis-dichlorobis(2,2′-bipyridyl-4,4′-dicarboxylic acid)ruthenium(II) to sensitize TiO_2 electrospun fibers for the degradation of phenazopyridine under UV and visible irradiation. Vinu et al. [14] used xanthene-fluorone dyes, Eosin Y (EY), and fluorescein (FL) dyes, to sensitize nano-TiO_2 for the degradation of phenolic compounds under visible light. Finally, Hamdi et al. [15] used chitosan (CS) as a template for the preparation of CS-phthalocyanine-TiO_2 composites able to photodegrade aniline. However, the existing practice of the dye-sensitized TiO_2 photocatalytic system has few drawbacks that need to be overcome. First, transition metal or organic metal complexes used as sensitizers are toxic and generally very expensive [16,17]. Second, the dye may leach out into the treated water or degraded, producing side products which are need to be treated [6,14,16]. In addition, the regeneration, recovery, and reusability of the dye-sensitized TiO_2 in slurry mode remains a major problem for large-scale applications [16,17].

Our group has been working with immobilized photocatalysts for the past few years, particularly on TiO_2/CS layer-by-layer arrangement [5,22,23]. It was observed that upon light irradiation, the ENR_{50} in the TiO_2 formulation degraded and formed macro-pores within the surface of TiO_2 layer [22]. The macro-pores increased the surface area of the photocatalyst and improved the diffusion of pollutants and light penetration to the CS sub-layer, thereby enhancing the photocatalytic performance and reusability of the immobilized photocatalyst [22]. Furthermore, the immobilized TiO_2/CS photocatalyst has also shown improvement in the photocatalytic degradation of Reactive Red 4 (RR4) dye due to the synergistic effects of photocatalysis, adsorption, and self-sensitization processes [5]. The chemisorbed RR4 dye at the CS sub-layer has the capability of participating in the electron transfer process to improve the photocatalytic decolorization of RR4 dye in the bulk solution.

The main objective of this work is to explore the potential of immobilized TiO_2/CS loaded with RR4 dye in a layer-by-layer arrangement (TiO_2/RR4-CS/glass) for the photocatalytic degradation and mineralization of phenol. Phenol was chosen as a model pollutant since it does not have adsorption ability towards the TiO_2/CS photocatalyst [22]. Therefore, any enhancement in the photocatalytic activity would prove the sensitization effect by the chemisorbed dye. The RR4 dye is a highly stable tetrasulfonated monoazo dye that is commonly used in textiles and dyestuff industries. It is metal-free, cheap, and commercially available. Considering that the industrial textile wastewater consists large amount of dyes, these dyes can be recycled and use as an effective dye sensitizer in wastewater treatment, solar cells or hydrogen generation.

2. Experimental section

2.1. Materials

Chitosan (CS) flakes (68.2% degree of deacetylation with a molecular weight of 322 g mol^{-1}), Reactive Red 4 (RR4) dye with 50% dye content (color index number: 18,105, chemical formula: $C_{32}H_{23}ClN_8Na_4O_{14}S_4$, molecular weight: 995.23 g mol^{-1}, λ_{max}: 517 nm), terephthalic acid (TA, 98%), and TiO_2 (99% anatase) were purchased from Sigma-Aldrich (USA). Other chemicals used were epoxidized natural rubber (ENR_{50}) (Kumpulan Guthrie Berhad), ethylenediaminetetraacetic acid (EDTA) di-sodium salt (Ajax Chemicals, Australia, 99%), *p*-benzoquinone (BQ) (BDH Chemicals Ltd., UK, 98%), phenol (Scharlau, Spain, 99.5%), and phenol formaldehyde (PF) powder resin (Borden Chemical (M) Sdn. Bhd., Malaysia, 99%). All chemical solutions were prepared using ultra-pure water (resistivity = 18.2 MΩ cm).

2.2. Preparation of the immobilized photocatalysts

The preparation of the immobilized photocatalysts was previously described in detail elsewhere [5,23]. It involves three steps: (1) casting of CS solution, (2) adsorption of RR4 dye, and (3) dip-coating of TiO_2 formulation. The CS solution was prepared by grounding 6.0 g of CS flakes and 400 mL of 5% acetic acid in a ball mill grinder for 30 h. After the grounding process, the produced CS solution was casted evenly on the surface of glass plates (dimensions 4.7 × 6.5 cm) before air-dried at room temperature (27°C). Glass plates containing 0.65 ± 0.08 mg cm^{-2} of CS (with thickness of 6.15 ± 0.13 μm) were subjected to an adsorption process in RR4 dye solution. The concentrations of RR4 dye were monitored at a wavelength of 517 nm using a HACH DR/2000 (USA) direct reading spectrophotometer. The adsorption study of RR4 dye by the CS/glass had been reported in detail by Nawi et al. [23]. The adsorption capacity, q_e, of fully saturated RR4 dye on the CS sub-layer was calculated to be 172 mg g^{-1}. The dye-loaded CS (RR4-CS/glass) was washed with ultra-pure water to remove any non-adsorbed dye and then dried at room temperature before being coated with the TiO_2 formulation. The TiO_2 formulation was prepared by dissolving 5.0 g of ENR_{50} solution (~11.3% w/v of ENR_{50} in toluene), 0.15 g

of PF and 12.0 g of TiO_2 powder in 60 mL of acetone. The formulation was sonicated for at least 5 h before immobilizing the TiO_2 on the glass plates by a simple dip-coating technique. An optimum TiO_2 loading of 0.98 ± 0.08 mg cm^{-1} (thickness 14.5 ± 0.4 μm) [24] was used throughout this study. The immobilized photocatalysts were finally photo-etched under a 45-W compact fluorescent irradiation in ultra-pure water for at least 10 h before the photocatalytic reaction. The photo-etching process allows the degradation of unreacted polymers and increases the surface area of the immobilized TiO_2 photocatalyst [22,24–26]. The immobilized photocatalysts were hereafter called as TiO_2/glass, TiO_2/CS/glass, or TiO_2/RR4-CS/glass. An overview of the immobilized TiO_2/RR4-CS/glass photocatalyst is shown in Fig. 1.

2.3. Characterization

The optical absorption properties of the immobilized photocatalysts were examined by a UV–Vis diffuse reflectance spectroscopy (DRS) (Model Lambda 35, PerkinElmer, USA) within 200–800 nm using magnesium oxide (MgO) as the reference. Photoluminescence (PL) emission spectra were measured on a Jobin Yvon Horiba HR 800 UV spectrofluorimeter at an excitation wavelength (λ_{ex}) of 325 nm.

2.4. Experimental setup and procedures

The experiments were conducted in a lab-scale photocatalytic reactor and the setup was similar as reported elsewhere [5,23,24]. The reactor consists of a 45-W compact fluorescent lamp (Dicken Lighting, China) as the irradiation source, which was placed horizontally and in contact with the outer surface of a glass cell with dimensions of 5 × 8 × 1 cm. The lamp has a visible light irradiance (400–700 nm) of 490 W m^{-2} and a UV intensity (290–400 nm) of 4.0 W m^{-2}. A visible light irradiation was conducted by placing a UV filter (Contax, model L39UV) between the glass cell and the lamp. The immobilized photocatalysts were placed inside the glass cell with 20 mL of 10 mg L^{-1} phenol solution. Aeration was supplied throughout the reaction by using an aquarium pump (Hailea, model ACO-6603). The photocatalytic performance of the immobilized photocatalysts was also compared with the slurry TiO_2. This was done by suspending similar loading of TiO_2 powder as that of the immobilized TiO_2 layer in phenol solution. All the experiments were carried out at neutral pH of 6.6 and at room temperature (27°C ± 2°C).

The concentrations of phenol were monitored using a high-performance liquid chromatography (HPLC) on a JASCO HPLC system consisting of a PU-1580 Intelligent HPLC pump equipped with a UV-1570 intelligent UV/vis detector (JASCO, Japan). A Supelcosil C18 reverse phase column (Supelcosil, 25 cm × 4.6 mm, 5 μm) was used for the chromatographic separation at 25°C. A mobile phase was pumped at a flow rate of 0.5 mL min^{-1}, which was made up of a mixture between methanol (chromatography grade) and ultra-pure water with a ratio of 60:40 v/v. At every 20 min interval, 0.5 mL of sample were syringed out from the reaction mixtures and monitored at a wavelength of 220 nm. The percentage of phenol remaining (%) was calculated using the following equation:

$$\text{Phenol remained} = \left(\frac{C_t}{C_0}\right)100 \quad (1)$$

where C_t and C_0 are the concentration of phenol at time t (min) and the initial concentration, respectively. Triplication of all experiments was conducted under identical conditions and the average results are reported.

2.5. Detection of hydroxyl radicals ($OH^{\bullet}$)

Terephthalic acid (TA) fluorescence probing technique [27] was adopted for the analysis of $OH^{\bullet}$ radicals generated from the immobilized photocatalysts. The TA solution was prepared by diluting the TA powder in a 2 × 10^{-3} M of NaOH aqueous solution in order to obtain a concentration of 5 × 10^{-4} M. The pH of the solution was adjusted to pH 7.0 after the TA powder was dissolved. The immobilized photocatalysts were then immersed in 20 mL of the TA solution and was irradiated for 2 h with a 45-W compact fluorescent lamp. After 2 h of reaction time, the sample was withdrawn from the solution and the latter was analyzed by a fluorescence spectroscopy (model LS-55, PerkinElmer, USA) to detect the hydroxylation product of TA, 2-hydroxyterephthalic acid (TAOH), which emits at 425 nm using an excitation wavelength of 315 nm.

2.6. Mineralization study

The mineralization rate of phenol by the immobilized photocatalysts was determined by total organic carbon (TOC) analysis using a Shimadzu TOC-V CPH/CPN analyzer, (Japan). Similar experimental setup was applied with some

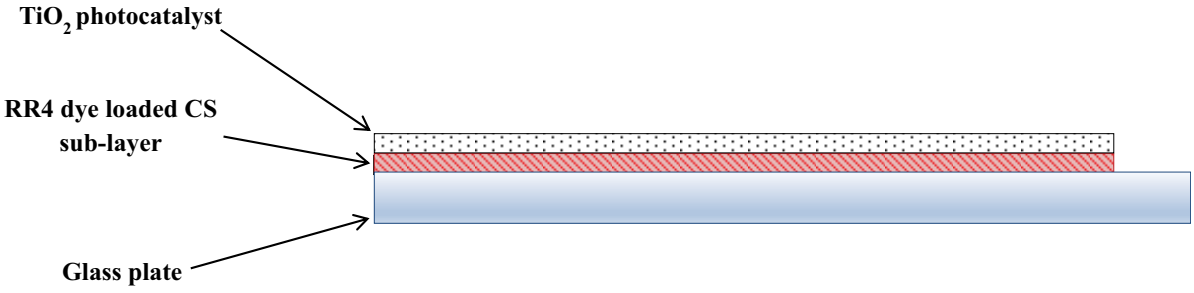

Fig. 1. Overview of the immobilized TiO_2/RR4-CS/glass photocatalyst.

modification. Longer glass plates and glass cell (dimensions 4.7 cm × 15 cm) were used to accommodate 50 mL of 10 mg L^{-1} phenol solution. About 10 mL of the sample was withdrawn from the solution after every 2 h interval and subjected to TOC analysis.

3. Results and discussion

3.1. Properties of RR4 dye

RR4 dye absorbs strongly in the UV (λ = 238 and 282 nm) and visible (λ = 517 nm) region (Fig. S1). It has a high absorbance coefficient, ε of 1.5 × 10^4 M^{-1} cm^{-1} at 517 nm [5], which is larger than that of Ru-complex photosensitizers [18,19], but lower than that of other organic dyes, such as Eosin Y, Erythrosin B, and Rose Bengal [28,29]. In addition, the energy level of the conduction band (CB) in TiO_2 ($E_{CB(TiO2)}$ = −4.2 eV) [30] is lower than the calculated energy level of the lowest unoccupied molecular orbital (LUMO) for RR4 dye ($E_{LUMO(RR4)}$ = −3.46 eV) [5]. Thus, the photogenerated electrons after the excitation of RR4 dye may transfer to the conduction band of TiO_2 [31]. In fact, the energy level of RR4 dye is almost similar to Eosin Y (−3.45 eV) and Rose Bengal (−3.55 eV) dyes [29]. Besides, IR absorption spectroscopy analysis shows that CS can strongly adsorb RR4 dye via electrostatic attraction between the amine groups of CS and sulfonic groups of RR4 dye [23]. The strong adsorption between the adsorbent–adsorbate allows the CS to be used as the substrate for the immobilization of the dye sensitizer.

3.2. Characterization of the immobilized photocatalysts

Fig. 2a shows the UV–Vis DRS spectra of the immobilized photocatalysts in the solid state. It demonstrates that the TiO_2/RR4-CS/glass has a strong and broad absorption band in the visible region due to the saturated concentration of RR4 dye which was around 5–7 wt.%. High concentration of the RR4 dye increased the emissions coming from the dye–dye interactions that resulted in the broadening of the band [32]. The presence of the RR4 dye should increase the photocatalytic activity of the TiO_2 photocatalyst in the visible region since the absorption bands of the TiO_2/glass and TiO_2/CS/glass are limited to the UV region only.

Photoluminescence (PL) was also used to determine the effect of RR4 dye on the recombination of electron–hole pairs. As shown in Fig. 2b, the immobilized TiO_2/glass, TiO_2/CS/glass, and TiO_2/RR4-CS/glass photocatalysts displayed broad band emission in the visible region within 400–550 nm, with two emissions at about 420 and 500 nm. The former is attributed to a band–band process, while the latter is ascribed to as an excitonic process caused by the surface oxygen vacancies and defects of the semiconductor [33]. All the immobilized photocatalysts showed no shift in the spectra with maximum emission at 500 nm. This indicates that incorporation of the RR4 dye does not significantly affect the properties of the semiconductor. Comparing the three immobilized photocatalysts, the TiO_2/glass exhibited the highest PL emission intensity, indicating that electron–hole pairs easily recombined [34]. On the other hand, the TiO_2/RR4-CS/glass materials exhibit the lowest emission intensity, indicating that the excited state of the RR4 dye sensitizer participates in the charge injection process [11]. The interfacial charge transfer process of the excited RR4 dye to the conduction band of TiO_2 inhibits the recombination of electron–hole pairs in TiO_2. The decrease of the recombination rate should increase the production of reactive oxygen species (ROS) and thus the photocatalytic activity of the TiO_2/RR4-CS material.

3.3. Evaluation of the photocatalytic performance

In order to evaluate the role of the dye sensitizer in the immobilized TiO_2 photocatalyst, a control test was conducted by comparing the photocatalytic performance of the TiO_2/RR4-CS/glass against the TiO_2/glass and TiO_2/CS/glass. The percentage of phenol remaining as a function of time using the immobilized TiO_2/glass, TiO_2/CS/glass, and TiO_2/RR4-CS/glass photocatalysts is shown in Fig. 3. In addition, control experiments involving photolysis and adsorption were also conducted.

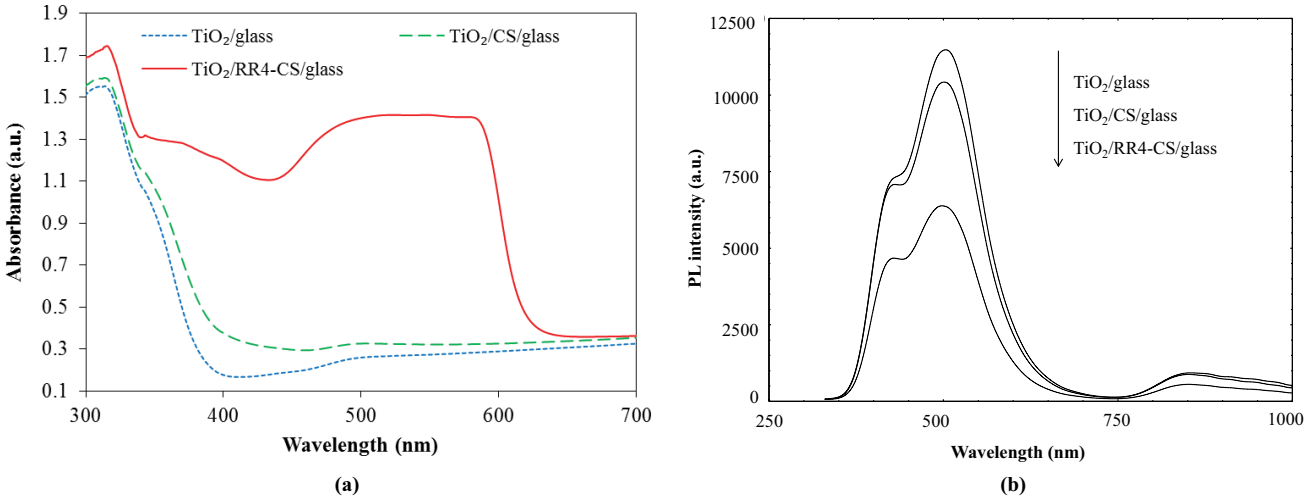

Fig. 2. (a) UV–Vis DRS and (b) PL spectra for the solid state of immobilized TiO_2/glass, TiO_2/CS/glass, and TiO_2/RR4-CS/glass photocatalysts.

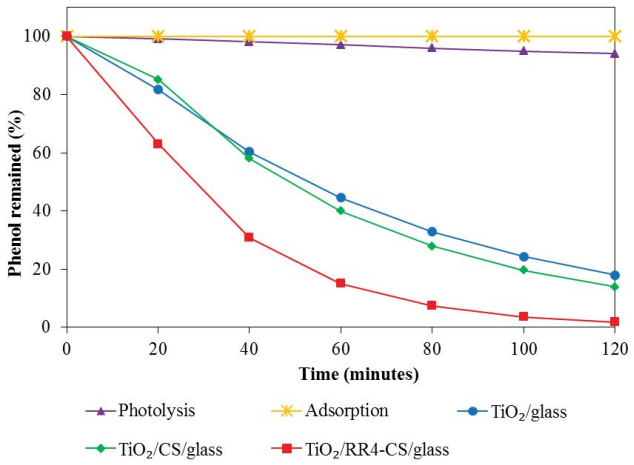

Fig. 3. Percentage of phenol remaining (%) as a function of time using the immobilized TiO_2/glass, TiO_2/CS/glass, and TiO_2/RR4-CS/glass photocatalysts at a pH of 6.6 with a TiO_2 loading of 0.98 mg cm^{-2} and an initial phenol concentration of 10 mg L^{-1}.

Phenol was weakly adsorbed at the surface of all photocatalysts and only 6.0% of phenol were photolyzed in the absence of the immobilized photocatalysts after 2 h of irradiation. This observation proved that both the adsorption and the photolysis processes can be neglected for the removal of phenol. The TiO_2/glass and TiO_2/CS/glass displayed 82.1% and 86.18% of phenol removal, respectively, under light irradiation after 2 h of reaction. Meanwhile, phenol could be completely removed under similar conditions by the TiO_2/RR4-CS/glass.

The pseudo-first-order rate constant, k (min^{-1}), was determined by the Langmuir–Hinshelwood kinetic model [35] and the equation is given by:

$$\ln\left(\frac{C_0}{C_t}\right) = -kt \quad (2)$$

where C_0 and C_t are the initial concentration of phenol and the concentration at irradiation time t (min), respectively. The k values were calculated from the linear slope plot of $\ln(C_t/C_0)$ vs. t and the results are shown in Table 1. Results show that the rate for the TiO_2/RR4-CS/glass was significantly higher than those calculated for other immobilized photocatalysts. The rate for the TiO_2/RR4-CS/glass was 0.030 min^{-1}, which was twice as fast as the TiO_2/glass and TiO_2/CS/glass. The high photocatalytic activity of the TiO_2/RR4-CS/glass can be attributed to its better photonic efficiency and to the deceased recombination of electron–hole pairs. Similar photocatalytic performance between the TiO_2/glass and TiO_2/CS/glass indicates that the CS sub-layer did not contribute to the removal of phenol. In this case, the phenol removal was only due to the photocatalytic performance of the TiO_2 top layer, since there was no occurrence of phenol adsorption by the CS sub-layer.

3.4. Mechanistic studies

In order to understand better the photocatalytic mechanisms and roles of different oxidative radicals, a comparison was made between the degradation curves of phenol by the immobilized TiO_2/RR4-CS/glass photocatalyst with those tested under a UV cut-off filter, N_2 gas and after the addition of specific radical quenchers (Fig. 4). Visible light irradiation was conducted under a UV cut-off filter in order to demonstrate the ability of chemisorbed RR4 dye to sensitize TiO_2. Visible light irradiation only generates weak amounts of electron–hole pairs in TiO_2 and thus sensitization should be dominant. The TiO_2/RR4-CS/glass shows 14.6% of phenol removal after 2 h under visible light irradiation. This observation explained the improved photocatalytic performance of TiO_2/RR4-CS/glass as compared with those by TiO_2/glass and TiO_2/CS/glass as discussed above. Both TiO_2/glass and TiO_2/CS/glass can only be activated under UV irradiation since their photoresponse is limited to the UV region. Therefore, high reaction rate achieved under light irradiation was due to two routes that run concurrently: (1) the major route by the TiO_2 itself by the small UV irradiance leakage from the light source and (2) the minor route by the dye sensitizer activated by visible light. The UV is generally responsible for enhancing the charge separation and the generation of oxidative species on the surface of TiO_2 photocatalyst, while the chemisorbed RR4 dye act as an electron donor to the conduction band of TiO_2. The degradation of phenol was completely suppressed when the photocatalytic reaction was carried out under N_2 gas. In the absence of dissolved O_2, the recombination rate of electron–hole pairs is

Table 1
Photocatalytic reaction constants of the immobilized TiO_2/glass, TiO_2/CS/glass, and TiO_2/RR4-CS/glass photocatalysts

Immobilized photocatalysts	Phenol degradation kinetic parameters	
	k (min^{-1})	R^2
TiO_2/glass	0.013	0.9887
TiO_2/CS/glass	0.015	0.9573
TiO_2/RR4-CS/glass	0.030	0.9865

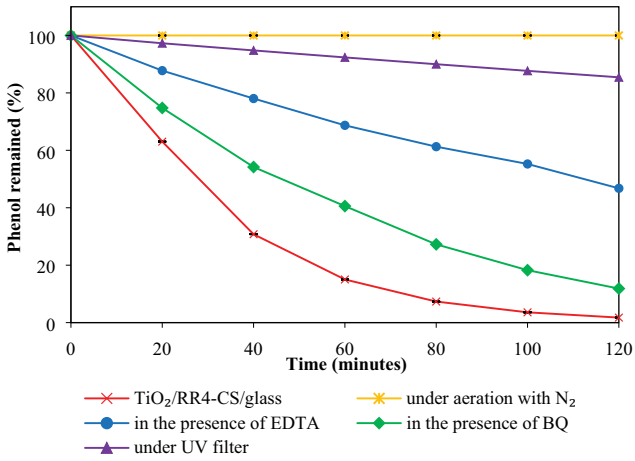

Fig. 4. Percentage of phenol remaining (%) as a function of time using the immobilized TiO_2/RR4-CS/glass photocatalyst under different conditions at a pH of 6.6 with a TiO_2 loading of 0.98 mg cm^{-2} and an initial phenol concentration of 10 mg L^{-1}.

greatly enhanced. Therefore, no oxidative radicals could be formed to promote the photocatalytic degradation. This indicates that the dissolved O_2 served as electron scavengers to reduce the recombination of electron–hole pairs and act as the key reactant to generate superoxide radicals as well as other reactive oxidative species. EDTA was also used during the phenol degradation process as a quencher of holes (h^+). In the presence of 1×10^{-3} M EDTA, the photocatalytic degradation of phenol decreased to 53.2%. This suggests that the predominant active oxidants responsible for initiating the degradation mechanism were the h^+ and/or $OH^\bullet$ species. When adding BQ, a quencher of superoxide radicals, only a slight decrease in the phenol degradation (88.1%) was observed even though dissolved O_2 was present.

The mechanisms of the immobilized TiO_2/RR4-CS/glass photocatalyst were further confirmed by the detection of $OH^\bullet$ radicals. Fig. 5 shows the fluorescence (FL) spectral changes of terephthalic acid (TA) solution after 2 h of irradiation time by the immobilized TiO_2/glass, TiO_2/CS/glass, and TiO_2/RR4-CS/glass photocatalysts. There was no FL peak observed in the reference sample (in the absence of light irradiation or photocatalysts). This indicates that the increase in FL intensity originates from the reaction between TA and $OH^\bullet$ radicals produced during the photocatalytic reactions. It was proven that under these experimental conditions, the hydroxylation reaction of TA proceeded mainly by $OH^\bullet$ radicals [27], without the interference from the photoinduced superoxide radicals ($O_2^{\bullet-}$), hydroperoxyl radicals ($HOO^\bullet$), and hydrogen peroxide (H_2O_2) [9]. Besides, the generated FL spectrum had the similar shape and maximum wavelength with that of a standard TAOH [27]. After 2 h of reaction, the TiO_2/RR4-CS/glass had the highest FL intensity which indicated that more $OH^\bullet$ radicals were generated by the photocatalyst. Almost similar FL intensities were obtained for TiO_2/glass and TiO_2/CS/glass, indicating that the same concentrations of $OH^\bullet$ radicals were produced by these photocatalysts. RR4 dye influenced the formation of $OH^\bullet$ radicals in the TiO_2/RR4-CS/glass and enhanced its photocatalytic performance as compared with the TiO_2/glass and TiO_2/CS/glass. Lower recombination of electron–hole pairs and higher formation of $OH^\bullet$ radicals promote the photocatalytic performance of the system. The results obtained by the TA experiment confirmed that the $OH^\bullet$ radicals were the main active species during the photocatalytic reactions.

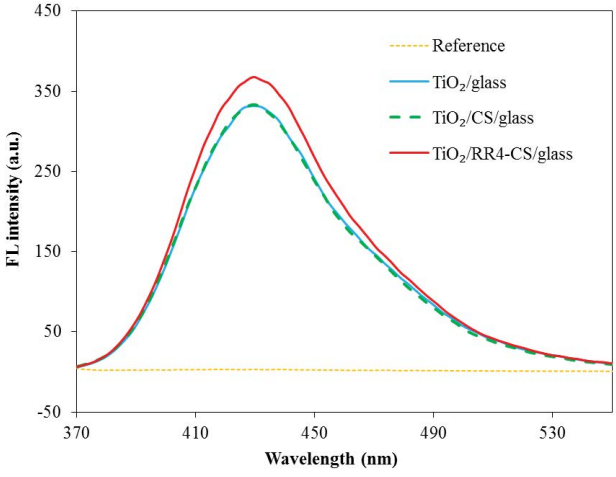

Fig. 5. Fluorescence spectra of TA solution after 2 h of irradiation using the immobilized TiO_2/glass, TiO_2/CS/glass, and TiO_2/RR4-CS/glass photocatalysts at a pH of 7.0 with a TiO_2 loading of 0.98 mg cm^{-2} (excitation wavelength = 315 nm).

Fig. 6 summarizes the overall mechanisms involved in the photocatalytic degradation of phenol by the immobilized TiO_2/RR4-CS/glass photocatalyst. It shows that the enhanced photocatalytic performance of the TiO_2/RR4-CS/glass was attributed to two routes, photocatalysis and sensitization, that run concurrently under light irradiation. When TiO_2 is excited by light (containing low UV intensity), the photoinduced holes (h^+) migrate to the surface of TiO_2 photocatalyst where they are scavenged by H_2O or OH^- ions to produce $OH^\bullet$ radicals. The phenol in the bulk solution was directly oxidized by the $OH^\bullet$. At the same time, as the chemisorbed RR4 dye absorbs visible light, its electrons will be excited from the highest occupied molecular orbital (HOMO) to the lowest unoccupied molecular orbital (LUMO). Since the energy level of RR4 dye satisfied for an electron transfer process to occur, the excited dye molecule (RR4*) will transfer its electrons into the TiO_2 conduction band. While the dye itself is converted to its cationic radical ($RR4^{+\bullet}$), the transferred electrons together with the photoinduced electrons (e^-) resulted in the accumulation of excess electrons in the TiO_2 conduction band. The electrons at the surface are scavenged by dissolved O_2 molecules to produce $O_2^{\bullet-}$, $HOO^\bullet$, H_2O_2, and especially $OH^\bullet$ radicals that are responsible for the degradation of phenol [35,36]. The $OH^\bullet$ and $O_2^{\bullet-}$ radicals may also attack the ground state dye and dye radical cations, respectively, which resulted in the degradation of the chemisorbed dye [14]. In addition, the transferred electrons could possibly undergo recombination with the dye radical cations to regenerate the dye in the ground state. These reactions, however, proceed at a slower rate as it competes with the electron transferred and electron scavenging reactions. This is evident by the reduction in the rate of phenol degradation under visible irradiation [13]. Better photoinduced charge carrier separation under light irradiation decreases the recombination of electron–hole pairs and enhanced the photocatalytic efficiency of the system.

3.5. Catalyst recyclability

The reusability of different immobilized photocatalysts was tested up to five consecutive experiments to measure the stability of the immobilized photocatalysts for the photocatalytic degradation of phenol. After each cycle, the immobilized photocatalysts were recovered, washed with ultra-pure water for 30 min and reused. The reusability of the immobilized photocatalysts is shown in Fig. 7 as a function of rate constants obtained in the photocatalytic degradation of phenol. In addition, the photocatalytic degradation of phenol by TiO_2 in slurry mode was also conducted for a comparison.

The results showed that the rate obtained by the TiO_2/glass and TiO_2/CS/glass remained almost constant from the first to the fifth cycles of their respective applications with the average rate values of 0.013 and 0.014 min^{-1}, respectively. These values are slightly lower than that obtained by TiO_2

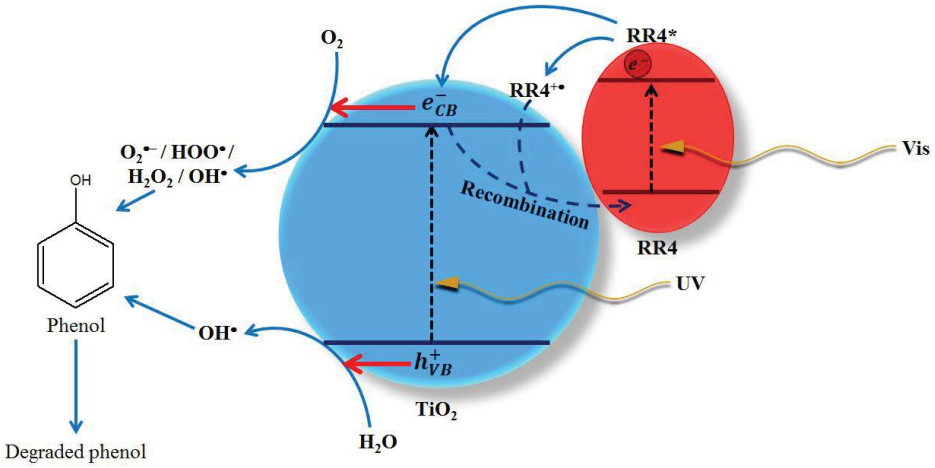

Fig. 6. Illustration of the possible mechanisms involved during the photocatalytic degradation of phenol using the immobilized TiO_2/RR4-CS/glass photocatalyst.

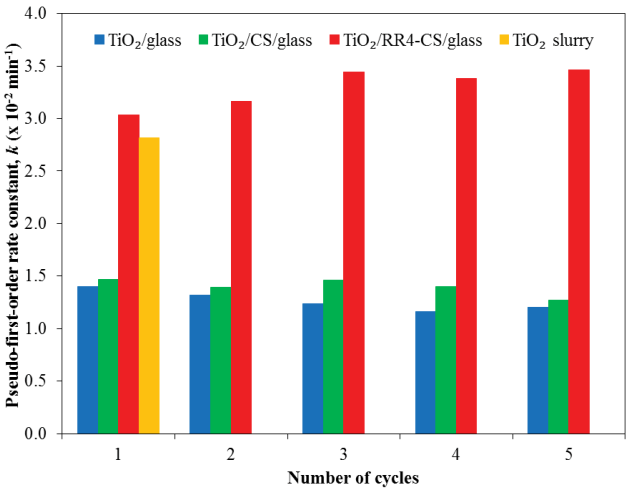

Fig. 7. A plot of pseudo-first-order rate constant of the immobilized photocatalysts as a function of consecutive cycles at a pH of 6.6 with a TiO_2 loading of 0.98 mg cm^{-2} and an initial phenol concentration of 10 mg L^{-1}.

in slurry mode whereby the rate obtained in the first cycle was 0.028 min^{-1}. However, the use of TiO_2 in slurry mode hindered the reusability of the photocatalyst. Based on Fig. 7, the TiO_2/RR4-CS/glass gives the best phenol degradation. Under the operation of this photocatalytic system, the average rate was 0.033 min^{-1}.

Although all the immobilized photocatalysts were practically reusable and sustainable in their photocatalytic applications, the rate of TiO_2/RR4-CS/glass was more than twofold higher than the TiO_2/glass and TiO_2/CS/glass. The excellent photocatalytic performance of the TiO_2/RR4-CS/glass originates from the sensitization effect of the chemisorbed RR4 dye. Most importantly, the TiO_2/RR4-CS/glass photocatalyst was reusable and highly stable under the studied conditions. Finally, there was no sign of dye desorption or leaching into the treated aqueous solution since the dye was strongly chemisorbed onto the CS sub-layer.

3.6. Regeneration of the immobilized TiO_2/RR4-CS/glass photocatalyst

During the photocatalytic reaction, the chemisorbed RR4 dye also undergoes oxidation. It was reported previously that the intensity of the RR4 color changes was more visible after repeated cycles of usage [5]. The RR4 color intensity decreases by 20.1% after the fifth cycles of application in ultra-pure water. The oxidation of RR4 dye caused deactivation of the immobilized photocatalyst upon reuse. Such a shortcoming can be overcome by re-adsorption with fresh dye on the spent photocatalyst. This is an added advantage of recycling dye waste. The spent photocatalyst was recovered after the fifth cycle and a fresh solution of the RR4 dye was re-adsorbed.

Fig. 8 shows the reusability of fresh and regenerated immobilized TiO_2/RR4-CS/glass photocatalyst for the photocatalytic degradation of phenol. The results show that the regenerated TiO_2/RR4-CS/glass showed ~22% lower photocatalytic efficiency as compared with the fresh photocatalyst. This result was primarily due to the insufficient amount of RR4 dye adsorbed in the regenerated samples (the adsorption capacity of adsorbed RR4 dye on the CS decreased from 172 to 30 mg g^{-1}) that can be oxidized as a sensitizer. This in turn decreases the number of electrons being transferred to the TiO_2 conduction band under the same light irradiation and consequently decreases the amount of oxidative species generated by the photocatalyst. However, the photocatalyst regained its photocatalytic efficiency and was reusable for at least five more cycles. This evidence suggests that the immobilized TiO_2/RR4-CS/glass photocatalyst can easily be regenerated by a simple and cost-effective method.

3.7. Mineralization study

The mineralization rate of phenol by the immobilized TiO_2/glass, TiO_2/CS/glass, and TiO_2/RR4-CS/glass photocatalysts was monitored by TOC analysis. Fig. 9 shows that the trend of phenol mineralization by the immobilized TiO_2/glass, TiO_2/CS/glass, and TiO_2/RR4-CS/glass photocatalysts

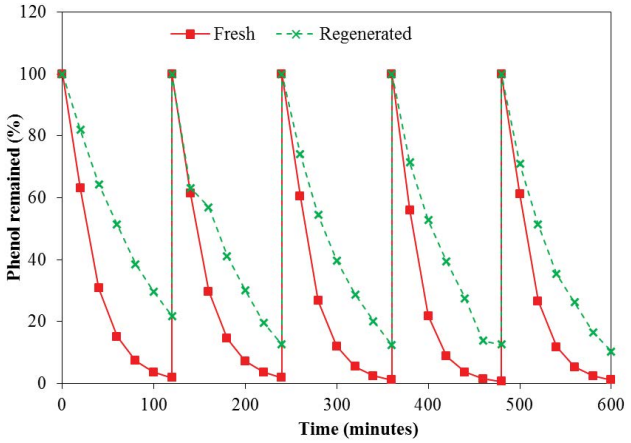

Fig. 8. Reusability of the fresh and regenerated immobilized TiO_2/RR4-CS/glass photocatalyst on the photocatalytic degradation of phenol at a pH of 6.6 with a TiO_2 loading of 0.98 mg cm^{-2} and an initial phenol concentration of 10 mg L^{-1}.

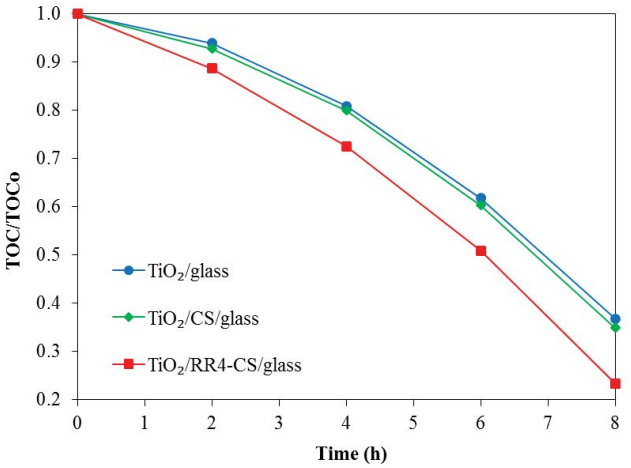

Fig. 9. TOC analysis of the immobilized photocatalysts as a function of mineralization rates of 50 mL phenol solution at a pH of 6.6 with a TiO_2 loading of 0.98 mg cm^{-2} and an initial phenol concentration of 10 mg L^{-1}.

was nearly identical throughout the reaction time, regardless of the pathways taken by each of the system. The TOC reduction was initially slow because at this stage the degradation of the phenol was initiated by branch dissociations with benzene rings still remained intact [37], producing intermediates such as catechol, *p*-benzoquinone, and hydroquinone as the first oxidation intermediates [38]. The mineralization rate of phenol by the TiO_2/RR4-CS/glass at this stage was faster than the TiO_2/glass and TiO_2/CS/glass due to the presence of the dye sensitizer. Therefore, more oxidative species could react with phenol and its intermediates leading to further oxidation of the by-products, yielding organic acids, such as maleic, oxalic, formic, and acetic [38].

After 4 h of reaction time, most of the phenol molecules were completely removed by the immobilized photocatalysts. Despite that, the mineralization rate of phenol by the TiO_2/glass, TiO_2/CS/glass, and TiO_2/RR4-CS/glass was much slower with a total mineralization of 63.2%, 65.1%, and 76.7%, respectively, after 8 h of reaction time. Longer irradiation time was needed to achieve complete mineralization. This could possibly due to the complicated reaction mechanisms of phenol oxidation. Overall, the TiO_2/RR4-CS/glass showed better photocatalytic performance for the mineralization of phenol with major intermediates previously identified as hydroquinone, catechol, and maleic acid [24]. There are no traces of RR4 dye intermediates and inorganic ions detected in the treated phenol solution either by the UV–Vis, HPLC, or ion chromatographic analyses. This likely originates from the low amount of RR4 dye being oxidized during the reaction or due to the re-adsorption of the intermediates produced on the surface of the CS sub-layer.

4. Conclusion

In summary, an immobilized TiO_2/RR4 dye-loaded CS photocatalyst (TiO_2/RR4-CS/glass) was successfully prepared for the photocatalytic degradation of phenol under a 45-W compact household fluorescent light irradiation. Results from the UV–Vis DRS and PL demonstrated that electron–hole pairs recombination was reduced and the visible light absorption enhanced in the immobilized TiO_2/RR4-CS/glass photocatalyst. The photocatalytic degradation and mineralization of phenol by the TiO_2/RR4-CS/glass were obviously improved as compared with the TiO_2/glass and TiO_2/CS/glass. The enhanced photocatalytic performance of the TiO_2/RR4-CS/glass can be attributed to two routes, photocatalysis and sensitization, that run concurrently under light irradiation. Both processes contributed to lower recombination of the electron–hole pairs and to better photoinduced charge carrier separation. In addition, the immobilized photocatalyst also demonstrated excellent reusability and good stability.

Acknowledgements

The authors are grateful to the Universiti Sains Malaysia (USM) for supporting this project under the Research University Postgraduate Research Grant Scheme (USM-RU-PGRS, 1001/PKIMIA/842070) and the USM Fellowship granted to S. Sabar. The authors would also like to acknowledge the School of Chemical Sciences as well as Geochemistry and Environmental Remediation Research Group (GEoRGe), USM for encouraging the collaboration with Université de Lorraine (UL).

References

[1] D. Wang, Y. Sun, Q. Shang, X. Wang, T. Guo, H. Guan, Q. Lu, Effects of the conjugated structure of Fe–bipyridyl complexes on photoinduced electron transfer in TiO_2 photocatalytic systems, J. Catal., 356 (2017) 32–42.
[2] E. Safaralizadeh, S.J. Darzi, A.R. Mahjoub, R. Abazari, Visible light-induced degradation of phenolic compounds by Sudan black dye sensitized TiO_2 nanoparticles as an advanced photocatalytic material, Res. Chem. Intermed., 43 (2017) 1197–1209.
[3] DOE, Environmental Quality (Sewage and Industrial Effluents) Regulations, Limits of Effluent Standard, Department of Environment, Ministry of Science, Technology and Environment, Malaysia, Petaling Jaya, Malaysia, 1974.

[4] M.R. Gogate, New paradigms and future critical directions in heterogeneous catalysis and multifunctional reactors, Chem. Eng. Commun., 204 (2017) 1–27.
[5] M.A. Nawi, S. Sabar, Sheilatina, Photocatalytic decolourisation of Reactive Red 4 dye by an immobilised TiO_2/chitosan layer by layer system, J. Colloid Interface Sci., 372 (2012) 80–87.
[6] S. Murphy, C. Saurel, A. Morrissey, J. Tobin, M. Oelgemöller, K. Nolan, Photocatalytic activity of a porphyrin/TiO_2 composite in the degradation of pharmaceuticals, Appl. Catal., B, 119–120 (2012) 156–165.
[7] N.M. Nghia, N. Negishi, N.T. Hue, Enhanced adsorption and photocatalytic activities of Co-doped TiO_2 immobilized on silica for paraquat, J. Electron. Mater., 47 (2018) 692–700.
[8] S. Rajoriya, S. Bargole, S. George, V.K. Saharan, P.R. Gogate, A.B. Pandit, Synthesis and characterization of samarium and nitrogen doped TiO_2 photocatalysts for photo-degradation of 4-acetamidophenol in combination with hydrodynamic and acoustic cavitation, Sep. Purif. Technol., 209 (2019) 254–269.
[9] Q. Xiao, L. Ouyang, Photocatalytic activity and hydroxyl radical formation of carbon-doped TiO_2 nanocrystalline: effect of calcination temperature, Chem. Eng. J., 148 (2009) 248–253.
[10] F. Laatar, H. Moussa, H. Alem, L. Balan, E. Girot, G. Medjahdi, H. Ezzaouia, R. Schneider, CdSe nanorod/TiO_2 nanoparticle heterojunctions with enhanced solar- and visible-light photocatalytic activity, Beilstein J. Nanotechnol., 8 (2017) 2741–2752.
[11] C. Su, C. Shao, Y. Liu, Electrospun nanofibers of TiO_2/CdS heteroarchitectures with enhanced photocatalytic activity by visible light, J. Colloid Interface Sci., 359 (2011) 220–227.
[12] N.N. Bahrudin, M.A. Nawi, Immobilized titanium dioxide/powdered activated carbon system for the photocatalytic adsorptive removal of phenol, Korean J. Chem. Eng., 35 (2018) 1532–1541.
[13] S.M. Boyer, J. Liu, S. Zhang, M.I. Ehrlich, D.L. McCarthy, L. Tong, J.B. DeCoste, W.E. Bernier, W.E. Jones Jr., The role of ruthenium photosensitizers in the degradation of phenazopyridine with TiO_2 electrospun fibers, J. Photochem. Photobiol., A, 329 (2016) 46–53.
[14] R. Vinu, S. Polisetti, G. Madras, Dye sensitized visible light degradation of phenolic compounds, Chem. Eng. J., 165 (2010) 784–797.
[15] A. Hamdi, S. Boufi, S. Bouattour, Phthalocyanine/chitosan-TiO_2 photocatalysts: characterization and photocatalytic activity, Appl. Surf. Sci., 339 (2015) 128–136.
[16] A. Zyoud, N. Zaatar, I. Saadeddin, M.H. Helal, G. Campet, M. Hakim, D. Park, H.S. Hilal, Alternative natural dyes in water purification: Anthocyanin as TiO_2-sensitizer in methyl orange photo-degradation, Solid State Sci., 13 (2011) 1268–1275.
[17] N. Hashim, S. Thakur, M. Patang, F. Crapulli, A.K. Ray, Solar degradation of diclofenac using Eosin-Y-activated TiO_2: cost estimation, process optimization and parameter interaction study, Environ. Technol., 38 (2017) 933–944.
[18] A. Islam, H. Sugihara, K. Hara, L.P. Singh, R. Katoh, M. Yanagida, Y. Takahashi, S. Murata, H. Arakawa, Sensitization of nanocrystalline TiO_2 film by ruthenium(II) diimine dithiolate complexes, J. Photochem. Photobiol., A, 145 (2001) 135–141.
[19] M.K. Nazeeruddin, A. Kay, I. Rodicio, R. Humphry-Baker, E. Mueller, P. Liska, N. Vlachopoulos, M. Graetzel, Conversion of light to electricity by cis-X2bis(2,2′-bipyridyl-4,4′-dicarboxylate) ruthenium(II) charge-transfer sensitizers (X = Cl-, Br-, I-, CN-, and SCN-) on nanocrystalline titanium dioxide electrodes, J. Am. Chem. Soc., 115 (1993) 6382–6390.
[20] N.S. Kumar, A. Dhar, A.A. Ibrahim, R.L. Vekariya, P. Bhadja, Designing and fabrication of phenothiazine and carbazole based sensitizers for photocatalytic water splitting application, Int. J. Hydrogen Energy, 43 (2018) 17057–17063.
[21] A. Tiwari, N.V. Krishna, L. Giribabu, U. Pal, Hierarchical porous TiO_2 embedded unsymmetrical zinc–phthalocyanine sensitizer for visible-light-induced photocatalytic H_2 production, J. Phys. Chem. C, 122 (2018) 495–502.
[22] M.A. Nawi, A.H. Jawad, S. Sabar, W.S.W. Ngah, Immobilized bilayer TiO_2/chitosan system for the removal of phenol under irradiation by a 45 watt compact fluorescent lamp, Desalination, 280 (2011) 288–296.
[23] M.A. Nawi, S. Sabar, A.H. Jawad, Sheilatina, W.S.W. Ngah, Adsorption of Reactive Red 4 by immobilized chitosan on glass plates: Towards the design of immobilized TiO_2-chitosan synergistic photocatalyst-adsorption bilayer system, Biochem. Eng. J., 49 (2010) 317–325.
[24] S. Sabar, M.A. Nawi, Fabrication and application of an immobilized TiO_2/chitosan layer-by-layer system loaded with Reactive Red 4 dye for the removal of phenol and its intermediates, Desal. Wat. Treat., 57 (2016) 10312–10323.
[25] M.A. Nawi, Y.S. Ngoh, S.M. Zain, Photoetching of immobilized TiO_2-ENR_{50}-PVC composite for improved photocatalytic activity, Int. J. Photoenergy, 2012 (2012) 12 p.
[26] M.A. Nawi, S.M. Zain, Enhancing the surface properties of the immobilized Degussa P-25 TiO_2 for the efficient photocatalytic removal of methylene blue from aqueous solution, Appl. Surf. Sci., 258 (2012) 6148–6157.
[27] K. Ishibashi, A. Fujishima, T. Watanabe, K. Hashimoto, Quantum yields of active oxidative species formed on TiO_2 photocatalyst, J. Photochem. Photobiol., A, 134 (2000) 139–142.
[28] W.J. Jones, A. Grofcsik, M. Kubinyi, D. Thomas, Concentration-modulated absorption spectroscopy and the triplet state: Photo-induced absorption/bleaching in erythrosin B, rose bengal and eosin Y, J. Mol. Struct., 792 (2006) 121–129.
[29] S. Min, G. Lu, Dye-cosensitized graphene/Pt photocatalyst for high efficient visible light hydrogen evolution, Int. J. Hydrogen Energy, 37 (2012) 10564–10574.
[30] Y. Xu, M.A.A. Schoonen, The absolute energy positions of conduction and valence bands of selected semiconducting minerals, Am. Mineral., 85 (2000) 543–556.
[31] A. Sergawie, S. Admassie, W. Mammo, T. Yohannes, T. Solornon, Synthesis and characterization of poly[3-(2′,5′-diheptyloxyphenyl)thiophene] for use in photoelectrochemical cells, Bull. Chem. Soc. Ethiop., 21 (2007) 405–417.
[32] M. Hu, Y. Xu, J. Zhao, Efficient photosensitized degradation of 4-chlorophenol over immobilized aluminum tetrasulfophthalocyanine in the presence of hydrogen peroxide, Langmuir, 20 (2004) 6302–6307.
[33] J. Liqiang, Q. Yichun, W. Baiqi, L. Shudan, J. Baojiang, Y. Libin, F. Wei, F. Honggang, S. Jiazhong, Review of photoluminescence performance of nano-sized semiconductor materials and its relationships with photocatalytic activity, Sol. Energy Mater. Sol. Cells, 90 (2006) 1773–1787.
[34] Y. Ku, Y.H. Huang, Y.C. Chou, Preparation and characterization of ZnO/TiO_2 for the photocatalytic reduction of Cr(VI) in aqueous solution, J. Mol. Catal. A: Chem., 342–343 (2011) 18–22.
[35] I.K. Konstantinou, T.A. Albanis, TiO_2-assisted photocatalytic degradation of azo dyes in aqueous solution: kinetic and mechanistic investigations: a review, Appl. Catal., B, 49 (2004) 1–14.
[36] J. Zhao, C. Chen, W. Ma, Photocatalytic degradation of organic pollutants under visible light irradiation, Top. Catal., 35 (2005) 269–278.
[37] C.H. Chiou, C.Y. Wu, R.S. Juang, Influence of operating parameters on photocatalytic degradation of phenol in UV/TiO_2 process, Chem. Eng. J., 139 (2008) 322–329.
[38] A. Rey, J. Carbajo, C. Adán, M. Faraldos, A. Bahamonde, J.A. Casas, J.J. Rodriguez, Improved mineralization by combined advanced oxidation processes, Chem. Eng. J., 174 (2011) 134–142.

Supplementary information

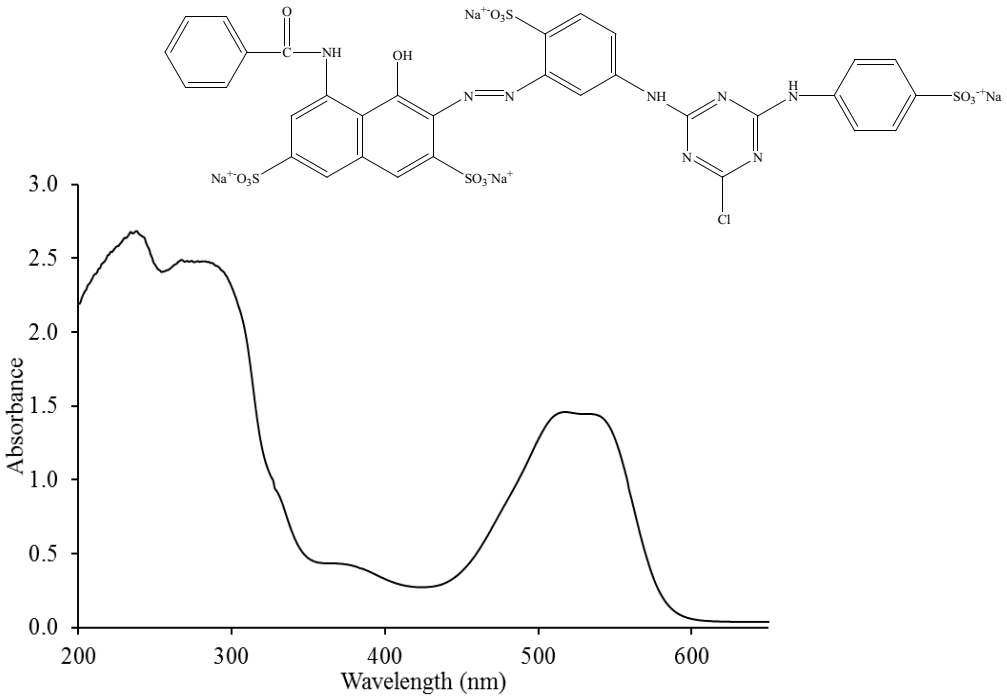

Fig. S1. UV–Vis DRS spectrum of the RR4 dye in ultra-pure water at neutral pH.